Journal of Magnetic Resonance **148,** 115–120 (2001)
doi:10.1006/jmre.2000.2224, available online at http://www.idealibrary.com on IDEAL®

Adiabatic TOCSY MAS in Liquids[1]

Ē. Kupče,*[,2] P. A. Keifer,† and M. Delepierre‡

*Varian Inc., 28 Manor Road, Walton-on Thames, Oxford KT12 2QF, United Kingdom; †Varian Inc., 3120 Hansen Way, Palo Alto, California; and ‡Laboratoire RMN, Institut Pasteur, 28 rue du Dr Roux, Paris, France

Received June 16, 2000; revised August 7, 2000

The effect of magic angle spinning (MAS) of liquids upon the performance of various isotropic mixing sequences is investigated. Although the mathematical formalism for isotropic mixing under MAS conditions is similar for both liquids and solids, the mechanism through which the coherence transfer is disturbed is different. In liquids, the use of sample spinning in the presence of both RF and magnetic-field inhomogeneities introduces a modulation of the effective field, which compromises the performance of the conventional mixing sequences. This effect is further amplified by supercycles, which normally improve the performance of the mixing and decoupling experiments. It is demonstrated that adiabatic mixing sequences are less susceptible to such modulations and perform considerably better in TOCSY MAS experiments. The best performance of TOCSY MAS is observed under the rotational resonance condition when the sample appears static in the nutation reference frame.

The small active volumes and the high sensitivities of Nanoprobes (*1*) make them ideal for applications where only a limited amount of sample is available. In such probes high sensitivity is achieved by maximizing the filling factor of the receiver coil. The line broadenings caused by the resulting magnetic susceptibility discontinuities are eliminated by using susceptibility-matched materials and by magic angle spinning (MAS), typically at 2- to 4-kHz speed. This use of MAS has the additional advantage of suppressing line broadenings in heterogeneous samples that have a nonuniform magnetic susceptibility across the sample, such as solvent-swollen resins (*2*, *3*). High resolution and high sensitivity allow routine liquid NMR experiments to be performed on a single bead of solid phase synthesis resins with typical sample quantities of under 500 pmol (*4*).

Although the vast majority of liquid-state NMR experiments can be recorded in Nanoprobes with no complications, in some cases interference effects have been observed (*5*). Particularly, performance of the conventional, composite-pulse 2D TOCSY experiment can be extremely poor and unstable (see Fig. 1a). On the other hand, the adiabatic TOCSY experiment (*6*) under the same conditions performs considerably better (see Fig. 1b).

In the course of this study we evaluated a number of standard liquid-state experiments at a wide variety of MAS rates. We verified that the signal-to-noise ratio was always practically independent of the MAS rate for those experiments that did not contain a spin-lock, for instance, NOESY, DQF–COSY, or simple spin-echo sequences. On the other hand, the performance of experiments employing recursive spin-lock sequences, such as isotropic mixing and spin decoupling, were very sensitive to the sample spinning speed (see Fig. 2a). The use of adiabatic spin-locks typically improved the overall quality of the data (see Fig. 2b). We also found that the magnitude of these effects strongly depended upon the sample volume, the sample geometry, and even the quality of shimming. Surprisingly, experiments that employ continuous wave spin-locks, for instance off-resonance ROESY (*7*) or selective cross-polarization experiments (*8*, *9*), seemed to be substantially less sensitive to variation of MAS speed.

Below we explore the effects of various spin-lock sequences on liquid samples spinning at the magic angle. It is demonstrated that the spin dynamics of experiments that employ repetitive sequences of composite pulses, such as isotropic mixing or spin decoupling, are least disturbed when the sample spinning speed is comparable to the spin nutation frequency. This condition is known as rotational resonance (*10*) in solid-state NMR, where it has found many useful applications.

The presence of rotational resonance in fast rotating liquids can be demonstrated by a simple nutation experiment (*11*). The 2D version of this experiment reveals the RF inhomogeneity in F_1 and magnetic field inhomogeneity in the F_2 dimension (see Fig. 3).[3] As shown in Fig. 3a the homogeneity of both the RF field and the magnetic field in a static sample is rather poor, partially because of somewhat casual sample shimming. This inhomogeneity is then largely removed by sample spinning at the magic angle (see Fig. 3b). However, if the RF field strength matches the spinning speed, a very sharp peak appears in the indirect dimension, as if the RF field was suddenly extremely

[1] Presented in part at the 41st Experimental NMR Conference, Asilomar, CA, April 10, 2000.

[2] To whom correspondence should be addressed. E-mail: eriks.kupce@varianinc.com.

[3] Strictly speaking, it is the inhomogeneity of the effective field, ω_{eff} that appears along F_1. Provided that ω_1 is much larger than the linewidth observed in F_2, $\omega_{\text{eff}} \approx \omega_1$.

1090-7807/01 $35.00

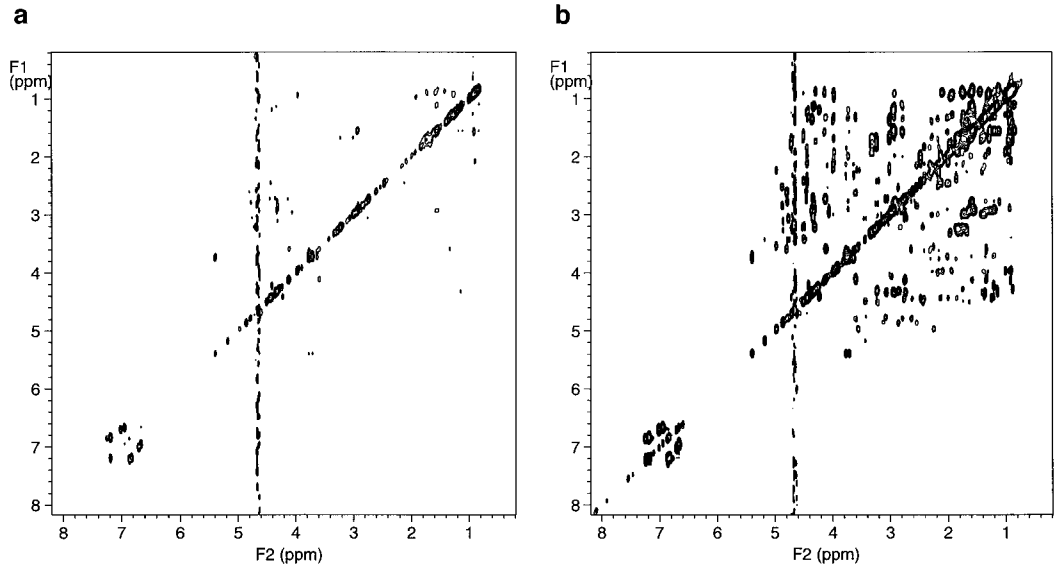

FIG. 1. Comparison of 2D H–H correlated *xy*-TOCSY spectra of a small protein (5) from scorpion venom (1 mM in D_2O) recorded at 500 MHz using a 40-μl sample in Varian's Nano-NMR probe at 2.5-kHz spinning speed; (a) composite pulse mixing (DIPSI-2), $B_{1max} = 6.94$ kHz, length of a single composite inversion pulse $T_p = 1.036$ ms; (b) adiabatic (WURST-2) mixing, $B_{1max} = 6.44$ kHz, length of a single adiabatic inversion pulse $T_p = 0.4$ ms. Both spectra were acquired using a 60-ms mixing time, 128 increments in t_1, and four scans per increment. The total experiment time for each data set was approximately 36 min.

homogeneous (see Fig. 3c). In fact, the magnetization does not dephase during this continuous wave spin-lock period because it is locked by the effective field (*11*), i.e., the magnetization follows the effective field in a manner similar to the adiabatic following (*12*). The broad component along the RF field axis in Fig. 3c comes from the parts of the sample where the rotational resonance condition is not met.

It is interesting to compare cross polarization (CP) in solids (*13–15*) with isotropic mixing in liquids (*16–19*). In both cases the spin dynamics can be described using the same formalism. The rotating-frame Hamiltonian is derived for an isolated *IS* spin pair,

$$H_{CP} = -\omega_{1I}I_x - \Delta\omega_I I_z - \omega_{1S}S_x - \Delta\omega_S S_z + \Im I_z S_z + H_{II}, \quad [1]$$

where ω_1 represents the RF field strengths as seen by the I and S spins, the $\Delta\omega$ terms are the corresponding resonance offsets, and H_{II} represents the homonuclear interactions. In solids the polarization transfer is achieved via the dipolar coupling ($\Im = b_{IS}$) whereas in liquids this process is mediated by the indirect (scalar) spin–spin coupling ($\Im = J_{IS}$). Assuming that $\omega_1 \gg \Im$ and ignoring the homonuclear interactions, the effective Hamiltonian in a tilted reference frame for a static sample is written

$$H_{eff} = -\omega_{eI}I_x - \omega_{eS}S_x + \Im_{eff}I_z S_z. \quad [2]$$

With the Hartmann–Hahn condition satisfied the first two terms in Eq. [2] vanish and the maximal polarization transfer can be achieved.

When the sample is spun at the magic angle, the heteronuclear dipolar coupling, b_{IS}, becomes time dependent:

$$b_{IS}(t) = \sum_k b_k e^{ik\omega_r t}. \quad [3]$$

This introduces the well-known "finger pattern" into the CP spectra as the Hartmann–Hahn condition splits into several subconditions:

$$\Delta = \pm k\omega_r, \quad [4]$$

where Δ is the RF mismatch parameter, k is an integer (usually $-2 \le k \le 2$), and ω_r is the spinning speed. The efficiency of CP in solids can be substantially improved by employing adiabatic B_1 field sweeps (*20–23*).

In liquids the scalar J_{IS} coupling is not directly affected by sample spinning. However, the effective fields seen by spins I and S are time dependent, in a manner similar to that for b_{IS} (see Eq. [3]). In order to show that such modulations can indeed affect the quality of spin-lock experiments, we simulated the influence of RF field modulation on the ability of various mixing sequences to return the starting magnetization to its initial state at the end of a single cycle. The result (see Fig. 4) reproduces the observations shown in Fig. 2 very well. As it appears from Fig. 4 and also from simulations not shown here, the composite pulse sequences are most vulnerable to sample spinning (*24*). This is hardly surprising, because the frequency spectrum of composite pulse sequences is particu-

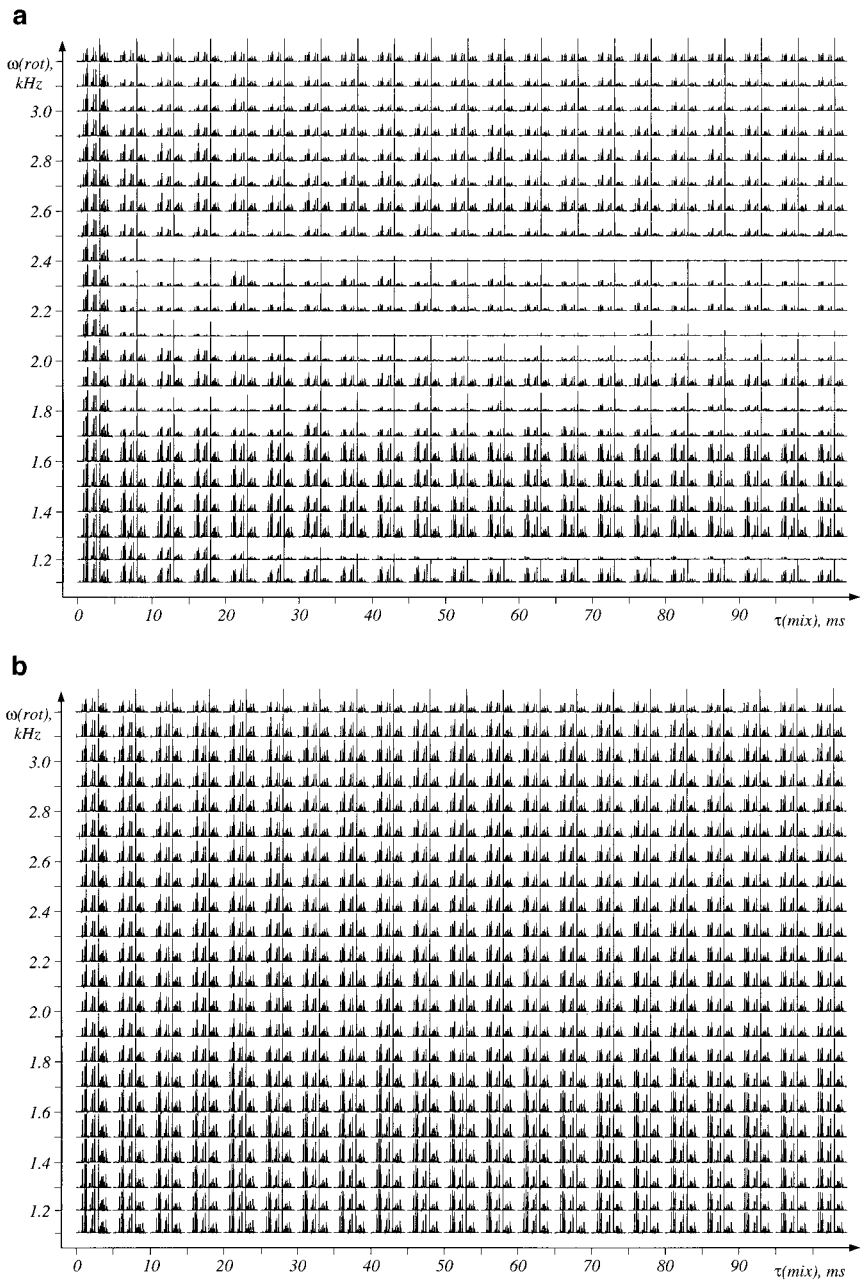

FIG. 2. Matrix plots of the first trace from H–H *z*-TOCSY spectra of 6 mg quinine in 40 μl CD_2Cl_2 recorded on INOVA 500 with gHX nanoprobe (a) using DIPSI-2 spin lock and (b) using WURST-2 spin lock. The vertical axis represents MAS spin rates ranging from 1100 to 3200 Hz (from bottom to top; in 22 steps of 100 Hz each). The horizontal axis shows increasing mixing times ranging from 0 to 100 ms (from left to right; in 21 steps of 5 ms each). No effort was made to synchronize the beginning of the experiment with the rotor position.

larly "noisy" (*25*) and additional modulation introduced by sample spinning destroys the delicate balance between individual RF field components created by numerical optimization. Additional simulations (not shown here) indicate that increasing the length of the initial 4-step MLEV-4 supercycle (*26*) to either MLEV-16 or a 20-step phase cycle (*27*, *28*) makes the performance of mixing sequences even more sensitive to rotation speed. Indeed, supercycles have been designed to work with inversion pulses that are all identical, whereas in the presence of sample spinning the performance of individual (composite) inversion pulses may vary substantially. As a result, at the end of the cycle the magnetization is not returned back to its initial state, as it would be in a static sample. For the same reason, the overall performance of the TOCSY experiment becomes increasingly sensitive to MAS speed as the length of a supercycle increases. Both the experimental data

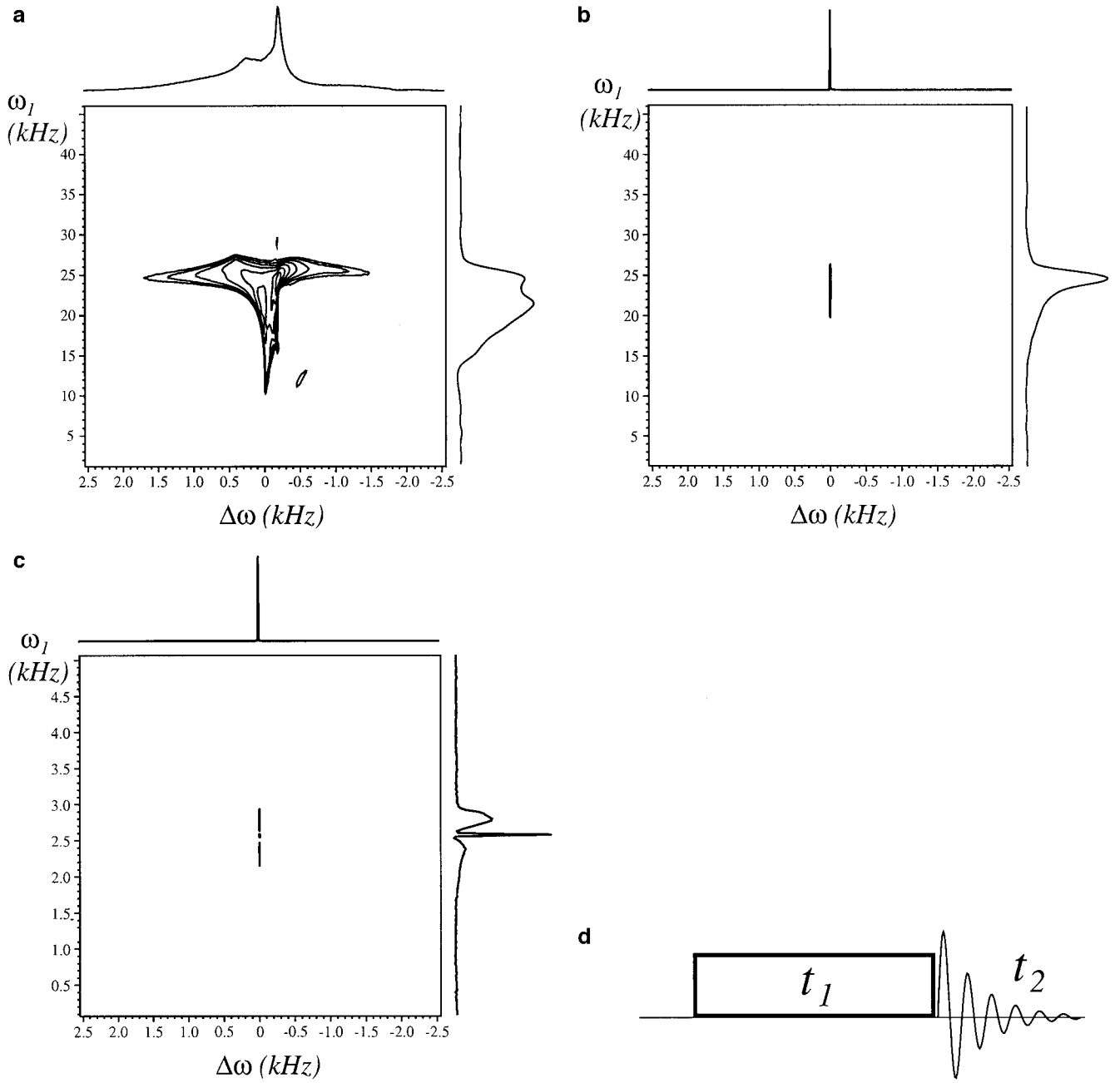

FIG. 3. The 2D nutation experiment recorded at 500 MHz in gHX nanoprobe using the H_2O sample. (a) Static sample, B_1 field strength of 25 kHz; (b) as in (a) but with sample spinning at the magic angle at 2.5-kHz speed; (c) the same as in (b) but using 2.5-kHz B_1 field strength. (d) The pulse sequence used to record the spectra. The sharp peak along the RF dimension (vertical) is due to the rotational resonance (see text). The broad component comes from parts of the sample where the rotational resonance condition is not met.

and the simulations also indicate that interference effects are stronger if the magnetization is in the *XY*-plane in the beginning of the spin-lock period.

Therefore, the optimum performance of isotropic mixing and spin decoupling can be expected if the length of individual inversion pulses, T_p, matches the rotor period, T_r, or its multiple (nT_r). Under these circumstances, in the reference frame rotating at a frequency of $1/T_p$ (nutation frame) the sample looks as if it is static and the individual contributions from ω_1 and $\Delta\omega$ modulation can be regarded as local distortions of the mixing field. As long as these distortions can be tolerated by the applied spin-lock sequence, the performance of the experiment is acceptable. Adiabatic pulses are known to be particularly insensitive to RF field distortions (*29*). Provided that the rotational resonance condition is met, the efficiency of spin mixing is further improved by supercycles.

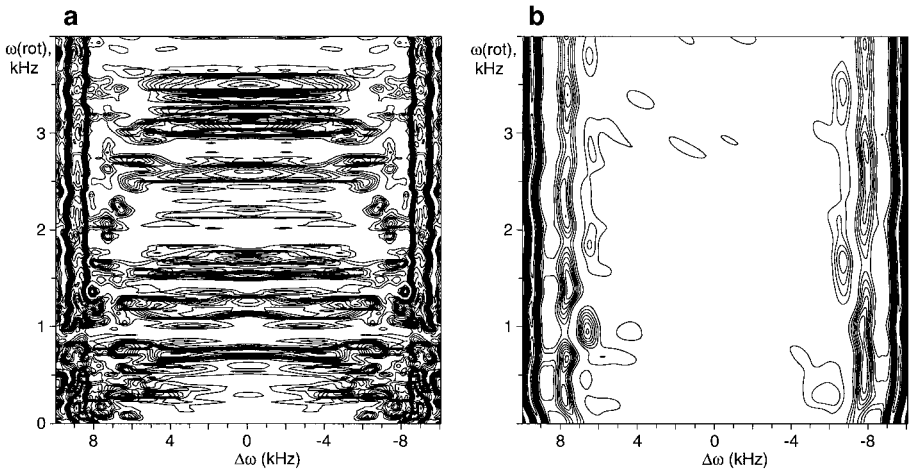

FIG. 4. Simulation of the effect of MAS upon the performance of (a) composite pulse (DIPSI-2, $T_p = 1.036$ ms) and (b) adiabatic (WURST-2, $T_p = 0.4$ m) spin lock. The 2D plots reveal the ability of the particular mixing sequence to return the magnetization to its initial state (M_z) after a complete MLEV-4 phase cycle. The amplitude of the RF field was modulated according to Eq. [3]. The evolution of magnetization was calculated by numerical integration of the ordinary Bloch equations (*12*). The modulation depth was 10% for the first harmonic and 5% for the second harmonic. The contour plots show residual M_z magnetization. The contour levels were increased linearly from 0 to 1 in steps of 0.1. Ideally, very little residual magnetization should be observed (see text).

For adiabatic spin locks the rotational resonance condition can be conveniently matched simply by adjusting the pulse length, T_p, to the rotor period, T_r. In the case of composite pulse mixing this may not always be feasible because the relation between the pulse length and the required RF field strength ($T_p \cdot B_1$) is fixed. Although both the experimental data and the simulations indicate the presence of other areas where the spin-lock performance is close to the optimal (see Figs. 2 and 4), they are typically less efficient and the relation to the MAS speed is not as obvious.

The interference effects from sample rotation can be minimized by reducing the influence of factors that cause the inhomogeneity of the effective field. For instance, use of susceptibility-matched materials for probe design and careful sample shimming reduce contributions from magnetic field (B_0) inhomogeneity. On the other hand, spherical or capillary samples designed to exploit only the most homogeneous parts of the probe also achieve the desired result. However, the probe filling factor in the latter case is reduced and so is the overall signal-to-noise ratio.

CONCLUSIONS

Although the appearance of interference between the Hartmann–Hahn polarization transfer and sample spinning is similar in solids and in liquids, the mechanisms affecting the experimental performance are quite different. The conventional composite-pulse mixing sequences are particularly vulnerable to such interference effects. The performance of TOCSY experiments can be substantially improved by using adiabatic (WURST-2) mixing sequences. The optimum performance in 2D TOCSY experiments is achieved under the rotational-resonance condition, when the repetition rate of the adiabatic pulses in a mixing sequence matches the MAS speed.

ACKNOWLEDGMENTS

We thank Tom Barbara, Knut Mehr, and Dave Rice from Varian Inc. (Palo Alto) for many useful discussions and suggestions.

REFERENCES

1. T. M. Barbara, *J. Magn. Reson. A* **109,** 265–269 (1994).
2. P. A. Keifer, L. Baltusis, D. M. Rice, A. A. Tymiak, and J. N. Shoolery, *J. Magn. Reson. A* **119,** 65–75 (1996).
3. P. A. Keifer, *Drugs Future* **23,** 301–317 (1998).
4. S. K. Sarkar, R. S. Garigipati, J. L. Adams, and P. A. Keifer, *J. Am. Chem. Soc.* **118,** 2305–2306 (1996).
5. M. Delepierre, A. Prochnicka-Chalufour, J. Boisbouvier, and L. D. Possani, *Biochemistry* **38,** 16756–16765 (1999).
6. Ē. Kupče, P. Schmidt, M. Rance, and G. Wagner, *J. Magn. Reson.* **135,** 361–367 (1998).
7. H. Desvaux, P. Berthault, N. Birlirakis, M. Goldman, and M. Piotto, *J. Magn. Reson. A* **113,** 47–52 (1995).
8. Ē. Kupče and R. Freeman, *J. Am. Chem. Soc.* **114,** 10671–10672 (1992).
9. S. N. Nicula, N. D. Kurur, and G. Bodenhausen, *J. Magn. Reson. A* **108,** 263–267 (1994).
10. T. G. Oas, R. G. Griffin, and M. H. Levitt, *J. Chem. Phys.* **89,** 692–695 (1988).
11. D. I. Hoult, *J. Magn. Reson.* **21,** 337–347 (1976).
12. A. Abragham, "The Principles of Nuclear Magnetism," Clarendon Press, Oxford, 1961.
13. S. R. Hartmann and E. L. Hahn, *Phys. Rev.* **128,** 2042–2053 (1962).
14. D. Marks and S. Vega, *J. Magn. Reson. A* **118,** 157–172 (1996).
15. X. Wu and K. W. Zilm, *J. Magn. Reson. A* **104,** 154–165 (1993).

16. L. Müller and R. R. Ernst, *Mol. Phys.* **38,** 963–992 (1979).

17. A. Bax, *Methods Enzymol.* **176,** 151–168 (1989).

18. M. H. Levitt, *J. Chem. Phys.* **94,** 30–38 (1991).

19. Z. L. Mádi, B. Brutscher, T. S. Herbrüggen, R. Brüschweiler, and R. R. Ernst, *Chem. Phys. Lett.* **268,** 300–305 (1997).

20. M. Baldus, D. G. Geurts, S. Hediger, and B. H. Meier, *J. Magn. Reson. A* **118,** 140–144 (1993).

21. S. Hediger, B. H. Meier, N. D. Kurur, G. Bodenhausen, and R. Ernst, *Chem. Phys. Lett.* **223,** 283–288 (1994).

22. D. E. Demco, H. Kostler, and R. Kimmich, *J. Magn. Reson. A* **110,** 136–145 (1994).

23. A. N. Garroway and G. C. Chingas, *J. Magn. Reson.* **38,** 179–184 (1980).

24. A. J. Shaka and J. Keeler, *Prog. NMR Spectrosc.* **19,** 47–129 (1987).

25. Ē. Kupče, J. Boyd, and I. D. Campbell, *J. Magn. Reson. A* **110,** 109–112 (1994).

26. M. H. Levitt and R. Freeman, *J. Magn. Reson.* **43,** 502 (1982).

27. R. Tycko, A. Pines, and J. Gluckenheimer, *J. Chem. Phys.* **83,** 2775 (1985).

28. T. Fujiwara and K. Nagayama, *J. Magn. Reson.* **77,** 53 (1988).

29. M. Garwood and K. Ugurbil, *in* "NMR Basic Principles and Progress" (J. Seeling and M. Rudin, Eds.), Vol. 26, pp. 109–147, Springer-Verlag, Berlin, 1992.